

## Introduction

Slough carbon, otherwise known as "dirt" in a reduction cell, can be defined as particles of carbon which have been loosened from the anode without being consumed electrolytically. These particles float on top of the bath and can degrade plant operations by:

1. Increasing operational costs due to increases in carbon consumption, since slough carbon is not consumed electrolytically.
2. Decreasing current efficiency, since a layer of slough carbon floating on the bath can act as an insulator and increase cell temperature.
3. Increasing the frequency of anode effects by decreasing the self-feeding rate of a cell from its crust.
4. Increasing labor costs due to the diversion of manpower required to skim pots.
5. Increasing plant operational costs due to the loss of bath material in skimmings.

Slough carbon is generally removed from a cell by either breaking open or in the more extreme cases, by skimming. We should mention that even during normal cell operation the slough carbon floating on the bath underneath the crust is oxidized to some extent by the  $\text{CO}_2$  produced electrolytically (the familiar Boudouard reaction,  $\text{C} + \text{CO}_2 \rightarrow 2\text{CO}$ ); although oxidation by  $\text{O}_2$  is much less rapid, and thereby less effective than oxidation by  $\text{O}_2$ . As for skimming a cell, this is not a desirable practice. Not only is it labor intensive as mentioned above, but also significant portions of bath are removed from the cell with the skimmings. It has been our experience that skimmings are actually only 5 to 25% carbon, the remainder being bath. Once this bath is removed from a cell, it is either lost or has to be reclaimed through some chemical treatment process to be reusable.

The mechanism by which slough carbon is generated is shown graphically in Figure 1 and generally accepted to be due to differences in the reactivities of the coked pitch (the binder) and the carbon aggregate(1-8). The pitch coke in a baked anode has a higher reactivity and is consumed during electrolysis (either chemically or electrochemically) at a more rapid rate than the aggregate. Therefore, pieces of aggregate on the exterior of the anode are left with few or no binder bridges attaching them to the bulk carbon phase. As a consequence, this aggregate can be dislodged from the anode and sloughed into the bath simply by mechanical agitation of the evolved  $\text{CO}_2$  bubbles. In support of these statements other authors have confirmed that slough carbon consists entirely of aggregate(4).

The difference in reactivity between binder and aggregate may very well be due to differences in their surface area. The binder phase has been shown to be responsible for the bulk of the surface area of baked anodes(3, 9-11). The surface area of either aggregate or coked pitch measured independently is not nearly so large as the surface area of the two combined in a baked anode(1). These results have been confirmed in our laboratory. Baked carbon anodes showed surface areas 5-10 times higher than either the aggregate or the coked pitch. This large increase arises during the baking process(10-13). As the baking temperature of an anode

## INFLUENCE OF BAKING TEMPERATURE AND ANODE EFFECTS

## UPON CARBON SLOUGHING

Euel R. Cutshall  
Reynolds Metals Company  
Reduction Laboratory  
P. O. Box 1200  
Sheffield, AL 35630

Vaughn L. Bullough  
Reynolds Metals Company  
Reynolds Carbon Division  
9428 Brookline Avenue  
Baton Rouge, LA 70809

Plant scale experiments involving prebaked anodes operating between 1.2 and 1.3 amp/cm<sup>2</sup> were conducted to determine the influence of anode effects and anode baking temperature upon carbon sloughing.

Our results support the evidence published in the literature that electrolytically generated  $\text{CO}_2$  is forced up through the interior of the anode and reacts most probably with the binder coke. As one approaches the working face of an electrolytically active anode, apparent density decreases and porosity, permeability and surface area increase.

However, this does not seem to be the major cause for carbon sloughing from this anode. The working face of all anodes tested was extremely hard and uniform. No carbon could be removed from the working face by rubbing one's fingers across it. The side of all of the anodes was much rougher, however, and carbon aggregate could easily be removed. This roughness could not have been caused by air burning, since the portion of the side of each anode considered was always below bath level.

Anode baking temperature has a large influence upon surface roughness. Poorly baked anodes had sides which were much rougher and had much looser aggregate than well baked anodes.

A single anode effect seems to have little influence upon surface roughness, and therefore, sloughing. However, multiple anode effects may very possibly cause an increase in carbon sloughing. This question could not be answered by the present work.

For this particular prebaked cell slough carbon is mainly generated on the sides of the anode. It would seem that there is a much smaller amount of slough carbon coming from the working face. This same conclusion should hold true for Soderberg anodes.

ries, the binder is shrinking. However, the aggregate generally being calcined at a higher temperature than that used during baking undergoes thermal expansion. The opposing forces resulting from binder shrinkage and aggregate expansion result in multitudinous small cracks (microcracks) forming in the binder. These microcracks are the element responsible for the large surface area of the baked anode.

But now the questions arise: What factors have the greatest influence upon sloughing and what can be done to minimize their negative contributions? When this work was initiated we felt that there were possibly three major factors which relate to sloughing:

1. Anode baking temperature
2. Cell current density
3. Anode effects

The purpose of this paper is to shed some light upon the contribution of two of these, anode effects and baking temperature, to carbon sloughing. Current density will be addressed in a later publication.

Prior research conducted in this area has shown that a portion of the  $\text{CO}_2$  produced electrolytically is forced up through the working face of an anode, primarily due to the hydrostatic pressure generated by the electrolyte (8, 10, 13, 14-16). This  $\text{CO}_2$  will react with the carbon inside the anode forming  $\text{CO}$ . It has been suggested that sloughing is entirely due to this  $\text{CO}_2$  penetration and subsequent reaction with interior carbon (10-11).

If this proposed model is correct, we should see decreases in density and increases in gas permeability, porosity and surface area for working anodes as we approach the working face from the inside of the anode. Also, the working face should be somewhat roughened and more friable than the remainder of the anode. The following material contains the results of experiments performed to evaluate this model.

#### Experimental Details

##### A. Baking

The first step, as with any experiment involving plant testing of anode blocks, was to obtain the blocks. Since block baking temperature was felt to be one of the variables which is critical to carbon sloughing, we had to measure the baking temperature of each block to be used in our experiments. We used Chromel-Alumel thermocouples bent at a  $90^\circ$  angle, and placed directly under the bottom face of each block, as shown in Figure 2.

We selected  $3/16"$  O.D. Inconel-sheathed Chromel-Alumel thermocouples; however, we soon learned that this thermocouple, by itself, would not stand up to the baking furnace environment due to the attack on the nickel in the Inconel sheath by sulfur released from the anodes during baking. Therefore, an additional protection tube surrounding the Inconel sheath was needed. Our final configuration consisted of the Inconel-sheathed Chromel-Alumel thermocouple as shown in Figure 2 surrounded by an  $1/8"$  steel pipe with a pipe cap on its lower end. All anodes were baked with this thermocouple configuration beneath them.

Maximum baking temperatures of all blocks were recorded as a function of time using a Fluke Model 2240B datalogger.

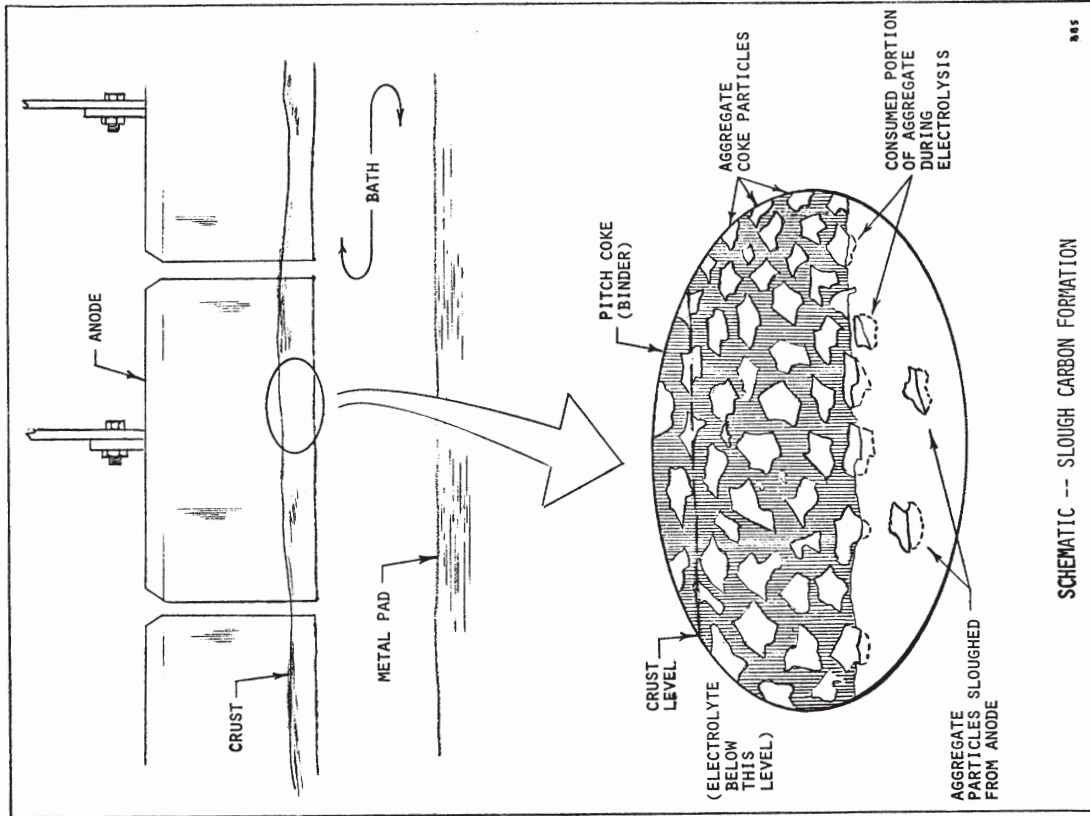


FIGURE 1.

Once the blocks were baked and cooled, they were removed from the pits and metal identification tags with the proper identification number attached to them. The blocks were then transferred to the potroom for use in our experiments.

**B. Electrolysis**

What we had in mind experimentally can be summarized as follows: Set four blocks in the same pot, electrolyze them for two days without an anode effect, monitor them to make sure they run at the same current density, pull two of them from the pot, allow the pot to go on light, and finally pull the two remaining blocks from the pot. The four blocks chosen for this experiment and their baking temperatures are listed below in Table I.

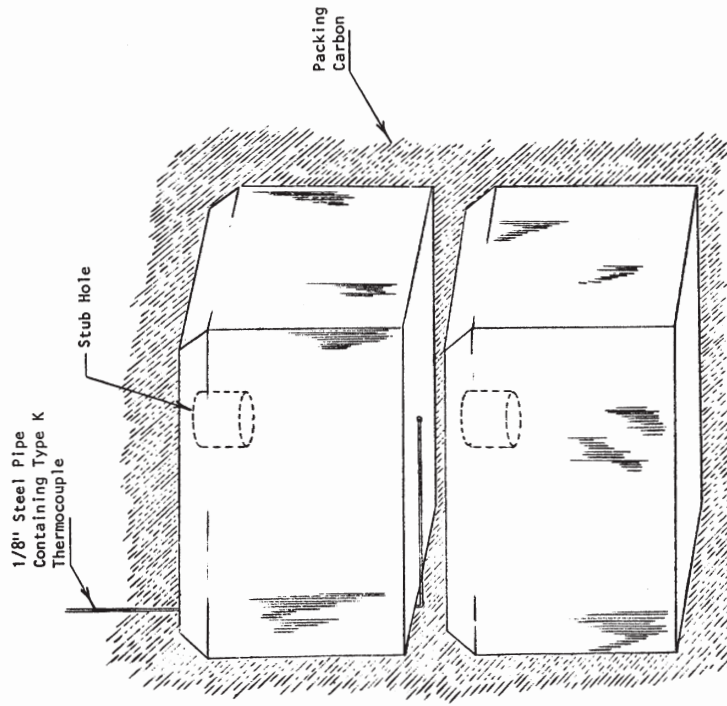
Table I. Anodes Used for Anode Effect Experiment

Block Number	Block Baking Temperature, °C
1	1090
2	1080
3	969
4	962

We used two high temperature blocks and two low temperature blocks. One block of each temperature range experienced an anode effect while the other block in the same range did not.

All four blocks were set and run in the same pot at the same time. After the first 8-10 hours of operation, the anodes reached their normal operating current density (1.3 amp/cm<sup>2</sup> or 8.4 amp/in<sup>2</sup>) which corresponds to 2700 amp per anode. Current density adjustments were made by changing the A-C distance of the anodes using a manual anode jack. Standard procedure was to make a change when necessary and then wait at least one-half hour before making another change. Current passing through the anode was measured directly using a Halmar digital clamp-on ammeter. This meter is an inductively coupled device which clamps around the anode stem and gives a direct digital readout of stem current. Readings were taken every 30 minutes. As a back-up means of measuring the current, voltage drops were measured across a 4 inch length of the copper stem. These readings, when coupled with temperature measurements of the stem, allowed us to calculate the stem current.

We attempted to operate each of the four anodes at 2700 amp; however, this amperage proved to be a problem. We could never seem to get all four operating stably without large swings up or down in amperage. As a result we decided to lower the amperage of all four to 2400 amp (1.2 amp/cm<sup>2</sup> or 7.7 amp/in<sup>2</sup>). Operation was much more stable at this level. Charts showing stem current as a function of time after setting each anode are given in Figures 3 through 6. As you can see all anodes operated at the same current density although the current was changed from 2700 to 2400 amp at approximately 24 hours into the experiment.



Note: Thermocouple is in direct contact with bottom of selected block.

THERMOCOUPLE PLACEMENT ON ANODE BLOCK IN BAKING PIT

FIGURE 2.

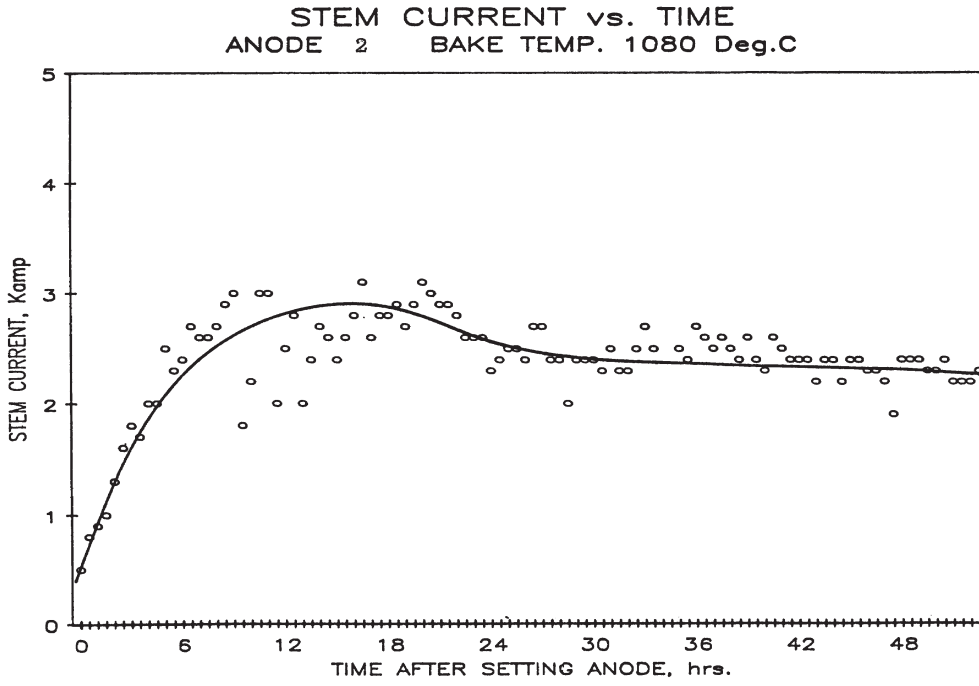


FIGURE 4.

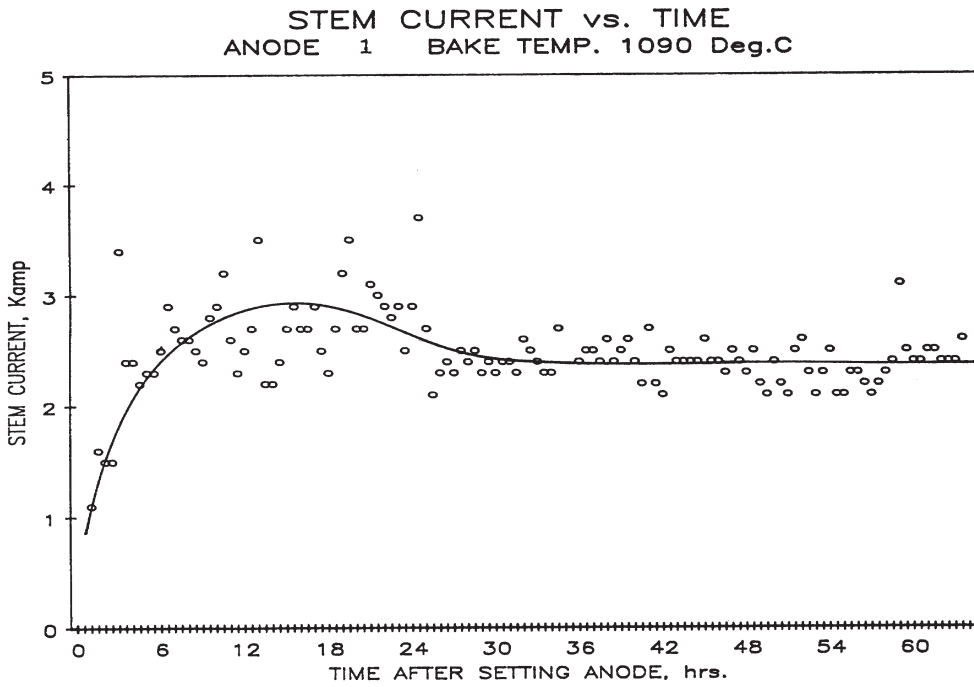


FIGURE 3.

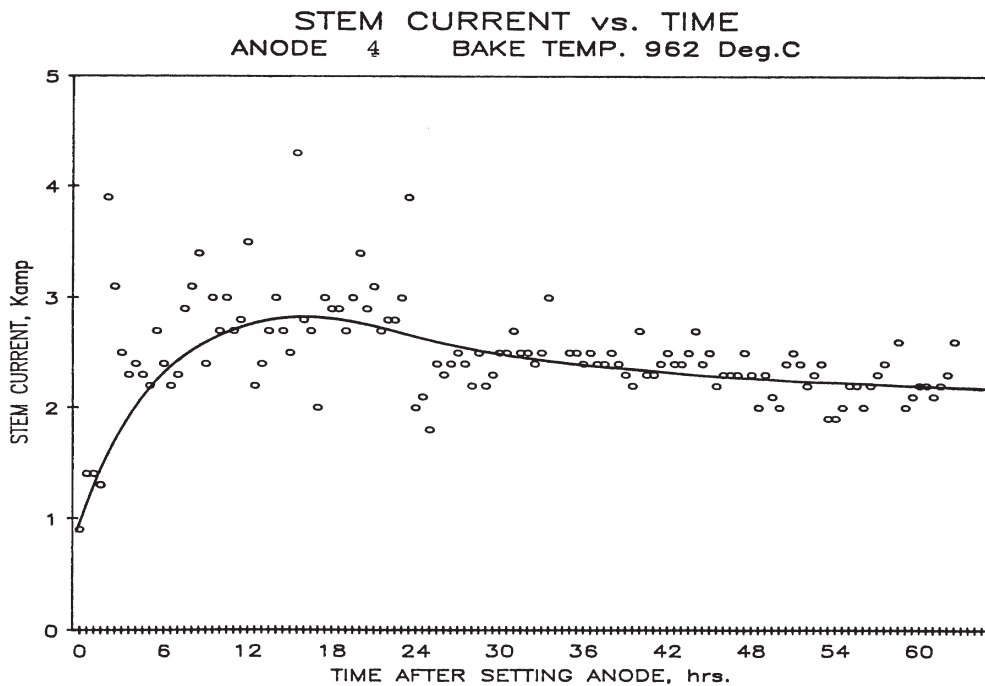


FIGURE 6.

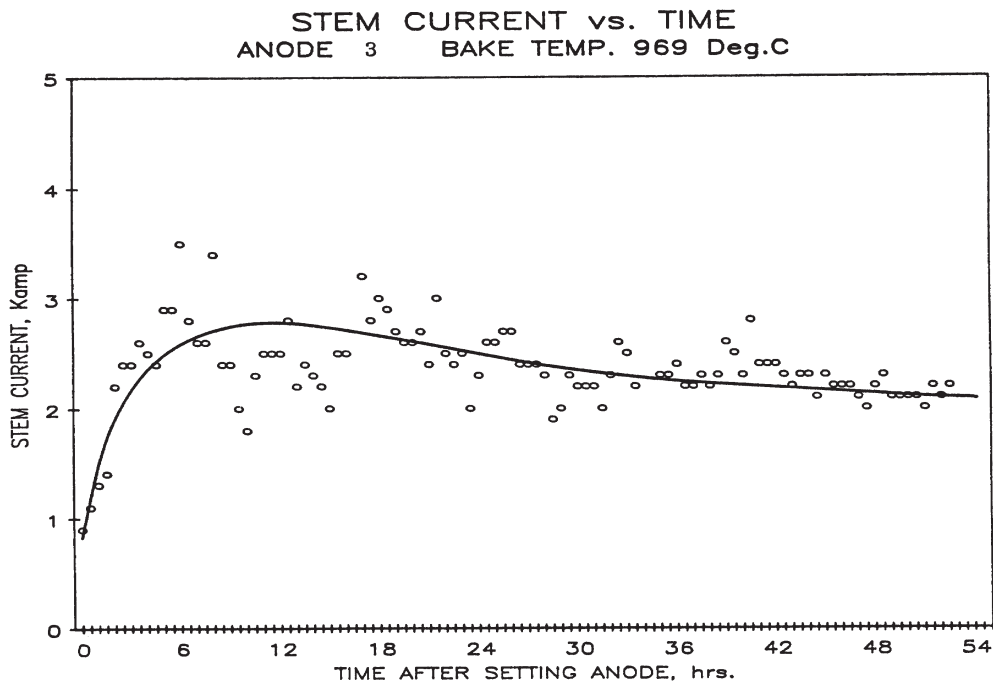


FIGURE 5.

At the end of two days of operation, anodes 2 and 3 were removed from the pot. Stem clamps were not loosened until the overhead crane was attached to the anodes and a slight upward tension applied. The anodes were pulled from the bath the moment the stem clamp was loosened to avoid bath penetration into the anode. In order to avoid air burning, we placed each anode, as soon as it was removed from the bath, in a closed steel box as shown in Figure 7, and flushed the box with argon until the anode had cooled to less than 200°C as measured by a thermocouple placed under it. No oxygen could penetrate the box due to the positive pressure of argon.

The alumina feed to the pot was then stopped and the pot was allowed to have an anode effect, the duration of which was 10 minutes. Immediately after quenching the anode effect, anodes 1 and 4 were pulled from the pot and cooled in an inert atmosphere as stated above. We should mention that quenching of the anodes in an inert atmosphere is a procedure of utmost importance in this experiment. If the anodes were not quenched but allowed to cool in the air and react with oxygen, we would not be measuring the consequences of electrolysis as we originally intended.

#### C. Analyses

Our approach to measuring the sloughing tendency of anodes was to determine the physical properties of the interior of the anode as a function of the distance above the anode electrolytic face. As a means of doing this each anode was cored as shown in Figure 8. The core, O.D. approximately 2.5 in., was extracted from the anode, machined to 2.0 in. O.D. and sliced into sections approximately 1 cm thick. The following physical properties were then determined for each section: Gas permeability, porosity, surface area and apparent density. A summary of the method used to determine each of these four properties is given in the Appendix. We felt that increases in permeability, porosity and surface area and decreases in apparent density of the sections as we approached the electrolytic face would indicate that CO<sub>2</sub> has permeated up through the anode, reacted with the interior anode carbon and increased the tendency for an anode to slough carbon into the bath.

In addition to using the anode interior properties as an indication of sloughing tendency, we have also determined a numerical index indicative of the surface roughness of the anode. Surface roughness of an operating anode is due to differences in reactivity of the binder coke and aggregate. The binder is consumed at a more rapid rate than the aggregate. This uneven consumption produces an irregular surface. The more uneven the surface, the greater the protrusions of aggregate and, therefore, the greater the amount of carbon sloughed into the bath.

Our method makes use of a flat aluminum plate 5.5 in. x 7.5 in. with 130 equally spaced holes in it. The plate is placed on the carbon surface and a depth gauge with a pointed probe measures the distance to the carbon surface. A total of 130 readings was taken for each surface. The average distance from the plate to the carbon was calculated along with its standard deviation. The mean tells us how far it is on the average from the highest aggregate "peaks" to the carbon surface. Likewise, the standard deviation indicates how much variation there is between the mean and the individual measurements.

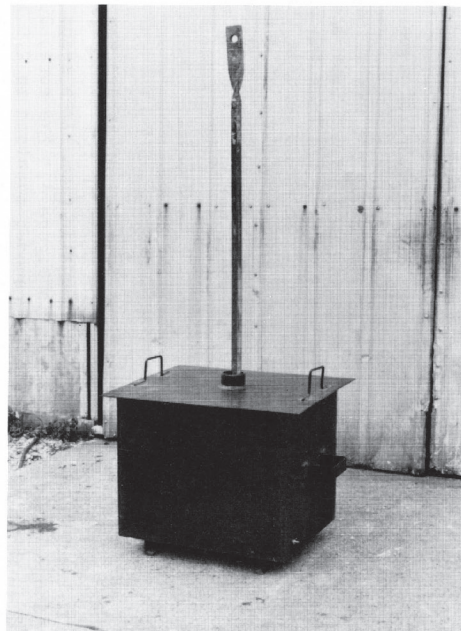
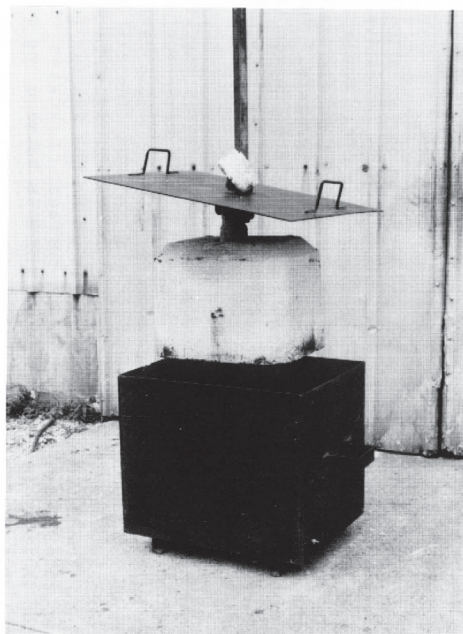


FIGURE 7.

#### ANODE QUENCH BOX

## Results and Discussion

This experiment was initiated to determine the relative importance of anode baking temperature and anode effects upon the sloughing process. We visualized CO<sub>2</sub> as penetrating the anode up through its working face and loosening aggregate carbon by preferentially reacting with binder coke. This aggregate would then be sloughed into the bath from the anode's working face. To test this hypothesis, we ran the aforementioned physical property tests on slices of cores and looked at changes in these properties with differing conditions of baking temperature and anode effects. The following section lists the data we obtained and the interpretation of the results.

A total of six anodes was cored and analyzed. Those anodes along with their operational conditions are listed below in Table II.

Table II. Experimental Anode Operating Parameters

Anode Number	Baking Temperature, °C	Anode Effect
1	1090	Yes
2	1080	No
3	969	No
4	962	Yes
5	1078	Not Electrolyzed
6	973	Not Electrolyzed

Note that the first four anodes are the ones listed in Table I. These were the four anodes which were electrolyzed. The remaining two anodes were not electrolyzed but were used as controls. Data from all six are listed in Tables III through VIII and shown graphically in Figures 9-20. In these figures all data are plotted as a function of the distance above the working face of the anode.

Apparent Density

First consider the control blocks in Figure 9, blocks which were baked but not electrolyzed. Baking temperature of one of the blocks was 973°C and the other was 1078°C. These represent our high and low bake temperature control blocks. You can see that the points for each block are dispersed with the points from the other block and that both sets of points can be represented by a single line. The apparent density of the blocks is constant above 5 cm, but below this value apparent density of each increases, due to the mechanics of forming the blocks inside the mold. However, this first 5 cm should have no effect upon the results of our experiment. This region of the block is consumed during the two days which each experimental block operated.

Now consider Figures 10 and 11. Figure 10 shows the influence of anode effects on blocks baked to a low temperature and Figure 11 does the same for blocks baked to a high temperature. In each figure (and, therefore, at each baking temperature) we see (1) a block which was operated in the cell for two days at its normal current density and which

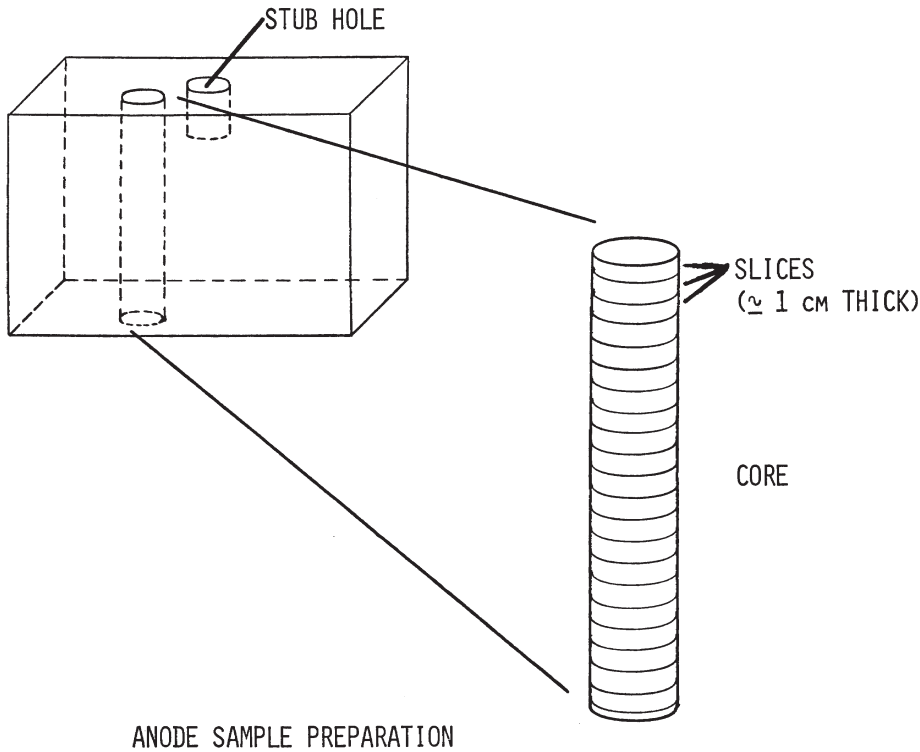


FIGURE 8.

TABLE III.  
PHYSICAL PROPERTIES - ANODE 1  
BAKING TEMPERATURE - 1090°C ANODE EFFECT - YES

Distance From Working Face, cm	Permeability, centidarcy	Apparent Density, g/cm <sup>3</sup>	Porosity, cm <sup>3</sup> /g	Surface Area, m <sup>2</sup> /g
0.69	8.34	1.45	0.150	1.07
1.90	7.25	1.45	0.146	1.04
3.12	6.36	1.47	0.127	1.09
4.31	6.00	1.49	0.127	1.01
5.51	6.09	1.48	0.138	1.04
6.69	6.48	1.48	0.141	1.05
7.85	5.67	1.49	0.132	0.97
8.96	5.38	1.50	0.115	0.92
10.12	4.79	1.52	0.127	0.81
11.29	5.29	1.51	0.122	0.82
12.46	6.00	1.50	0.109	0.77
13.62	5.02	1.51	0.119	0.76
14.60	5.49	1.50	0.128	0.57

TABLE IV.  
PHYSICAL PROPERTIES - ANODE 2  
BAKING TEMPERATURE - 1080°C ANODE EFFECT - NO

Distance From Working Face, cm	Permeability, centidarcy	Apparent Density, g/cm <sup>3</sup>	Porosity, cm <sup>3</sup> /g	Surface Area, m <sup>2</sup> /g
0.70	6.70	1.47	0.132	1.02
1.87	5.98	1.49	0.124	1.00
3.05	5.22	1.49	0.113	1.01
4.21	5.54	1.50	0.119	1.02
5.39	5.42	1.49	0.124	1.01
6.56	5.56	1.51	0.118	0.94
7.72	5.51	1.50	0.119	1.00
8.90	5.38	1.51	0.126	0.99
10.09	5.51	1.51	0.121	0.90
11.26	5.16	1.52	0.121	0.84
12.39	5.40	1.51	0.121	0.84
13.53	5.62	1.51	0.125	0.73
14.67	5.88	1.52	0.125	0.73

TABLE V.  
PHYSICAL PROPERTIES - ANODE 3  
BAKING TEMPERATURE - 969°C ANODE EFFECT - NO

Distance From Working Face, cm	Permeability, centidarcy	Apparent Density, g/cm <sup>3</sup>	Porosity, cm <sup>3</sup> /g	Surface Area, m <sup>2</sup> /g
0.94	8.35	1.46	0.141	3.06
2.13	5.28	1.51	0.123	3.46
3.29	4.73	1.52	0.128	2.46
4.43	5.54	1.52	0.121	1.66
5.53	4.40	1.53	0.113	1.23
6.71	4.32	1.54	0.124	1.03
7.88	3.97	1.53	0.112	0.82
9.06	4.47	1.53	0.111	0.82
10.22	5.69	1.51	0.113	0.85
12.50	4.52	1.52	0.118	0.78
13.62	3.53	1.55		
14.82	3.91	1.53	0.092	0.81

TABLE VI.  
PHYSICAL PROPERTIES - ANODE 4  
BAKING TEMPERATURE - 962°C ANODE EFFECT - YES

Distance From Working Face, cm	Permeability, centidarcy	Apparent Density, g/cm <sup>3</sup>	Porosity, cm <sup>3</sup> /g	Surface Area, m <sup>2</sup> /g
0.70	5.52	1.42	0.166	2.76
1.92	4.74	1.51	0.128	3.40
3.09	5.32	1.51	0.135	2.88
4.80	4.41	1.53	0.116	2.27
5.99	4.20	1.53	0.119	1.22
7.22	4.62	1.51	0.124	1.02
8.44	4.16	1.52	0.121	1.00
9.63	4.20	1.51	0.116	0.94
10.84	4.78	1.53	0.108	0.87
12.07	5.15	1.53	0.114	0.89
13.28	4.45	1.53	0.126	0.90
14.51	4.02	1.52		



TABLE VII.  
PHYSICAL PROPERTIES - ANODE 5  
BAKING TEMPERATURE - 1078°C  
NOT ELECTROLYZED

Distance From Working Face, cm	Permeability, centidarcy	Apparent Density, g/cm <sup>3</sup>	Porosity, cm <sup>3</sup> /g	Surface Area, m <sup>2</sup> /g
0.80	3.18	1.55	0.125	0.60
1.96	3.85	1.54	0.132	0.62
3.19	4.59	1.54	0.123	0.73
5.57	4.19	1.53	0.131	0.60
6.79	5.08	1.53	0.127	0.66
7.99	4.49	1.52	0.124	0.58
9.18	4.62	1.51	0.117	0.55
10.38	4.42	1.51	0.124	0.66
11.57	5.41	1.51	0.128	0.61
12.74	5.27	1.52	0.133	0.57

TABLE VIII.  
PHYSICAL PROPERTIES - ANODE 6  
BAKING TEMPERATURE - 973°C  
NOT ELECTROLYZED

Distance From Working Face, cm	Permeability, centidarcy	Apparent Density, g/cm <sup>3</sup>	Porosity, cm <sup>3</sup> /g	Surface Area, m <sup>2</sup> /g
0.70	3.86	1.57	0.097	1.78
1.93	3.66	1.55	0.112	0.78
3.12	3.71	1.53	0.113	0.87
4.33	4.78	1.52	0.112	0.76
5.52	4.78	1.52	0.108	0.78
6.73	5.05	1.53	0.106	0.83
7.94	4.95	1.52	0.113	0.77
9.14	4.89	1.53	0.108	0.80
11.92	4.15	1.53	0.107	0.77
13.13	4.34	1.52	0.114	0.81

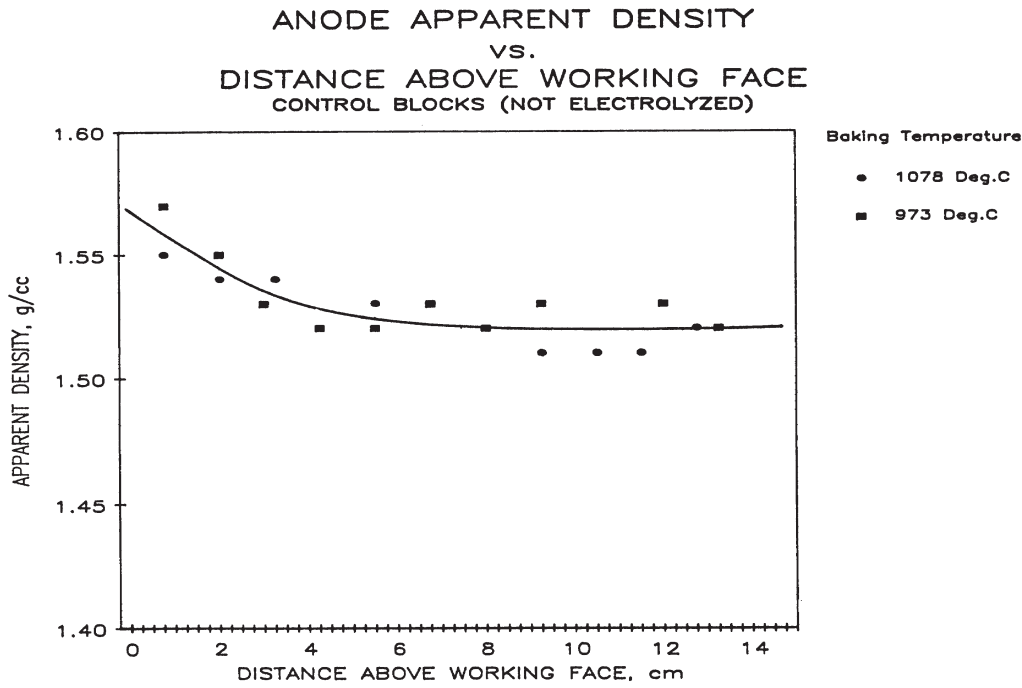


FIGURE 9.

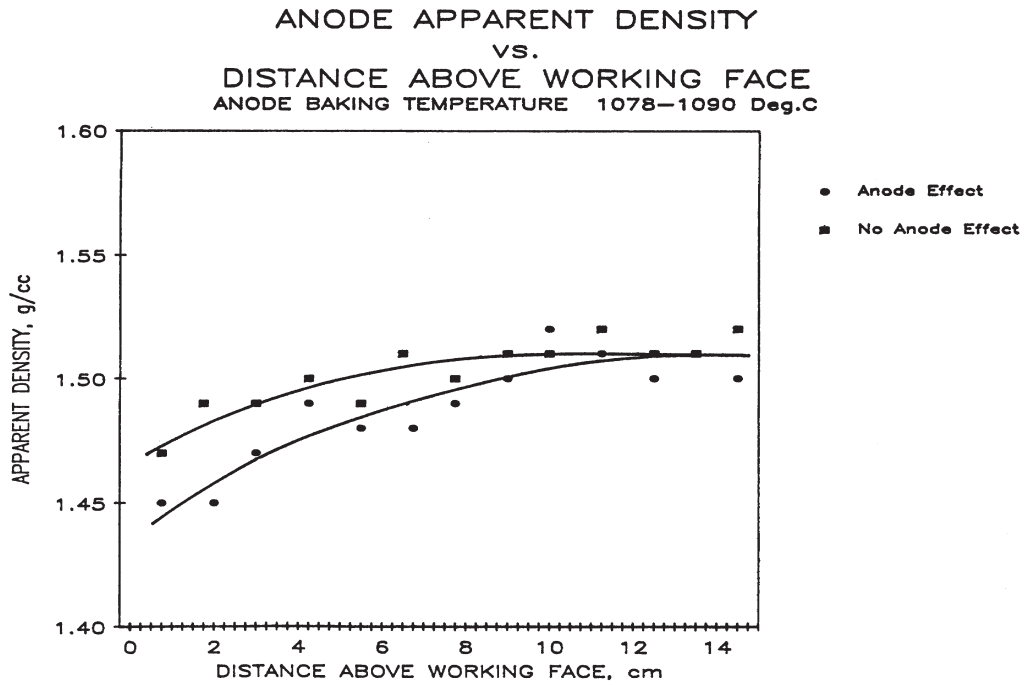


FIGURE 11.

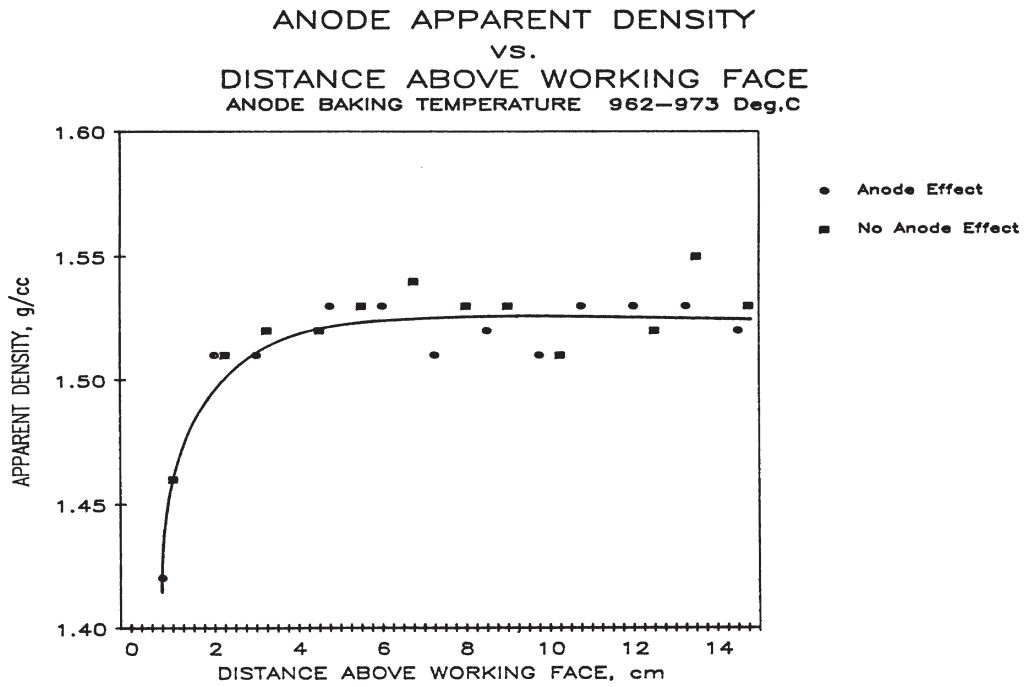


FIGURE 10.

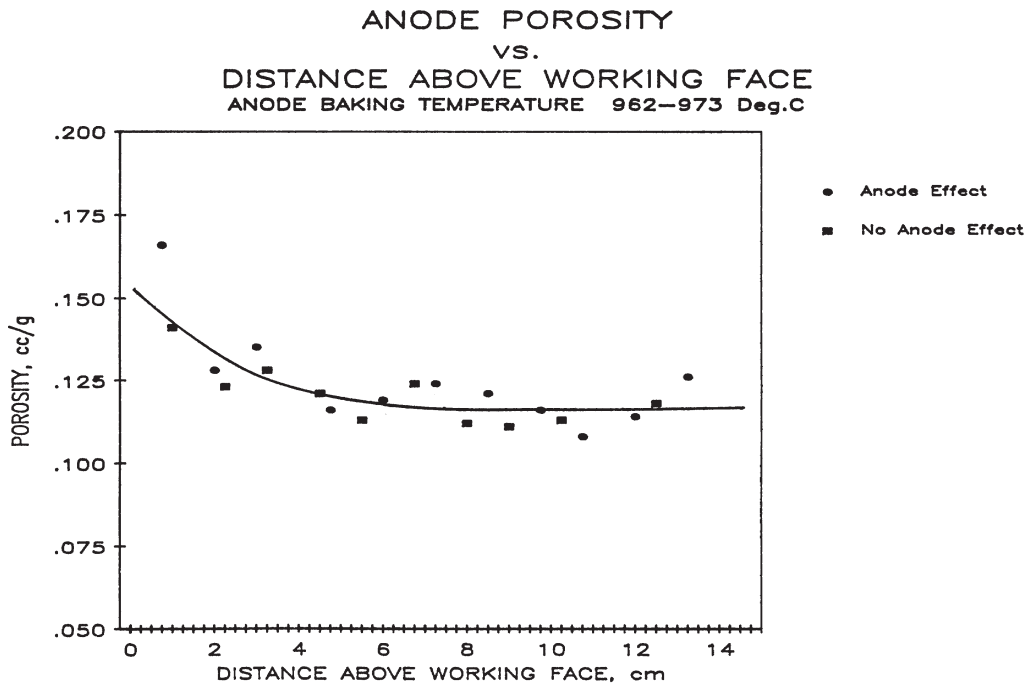


FIGURE 13.

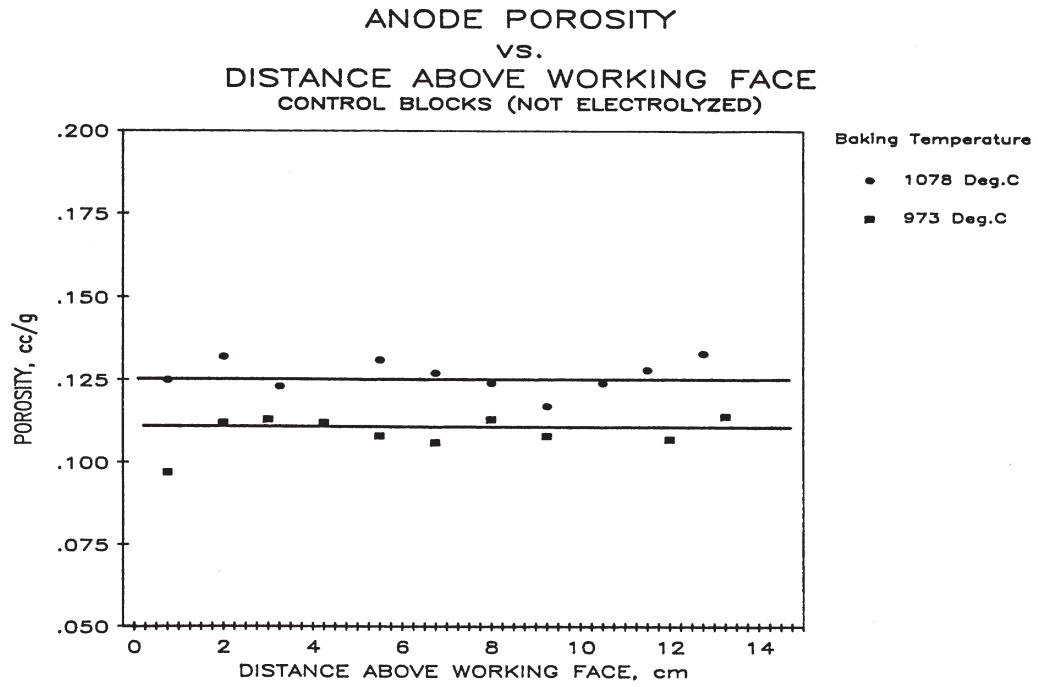


FIGURE 12.

ANODE PERMEABILITY  
vs.  
DISTANCE ABOVE WORKING FACE  
CONTROL BLOCKS (NOT ELECTROLYZED)

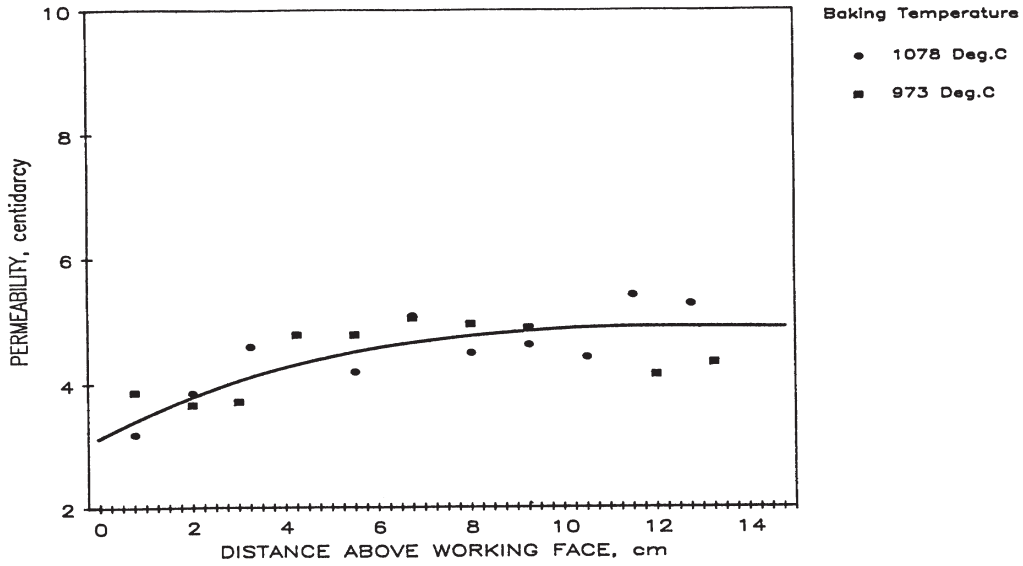


FIGURE 15.

ANODE POROSITY  
vs.  
DISTANCE ABOVE WORKING FACE  
ANODE BAKING TEMPERATURE 1078-1090 Deg.C

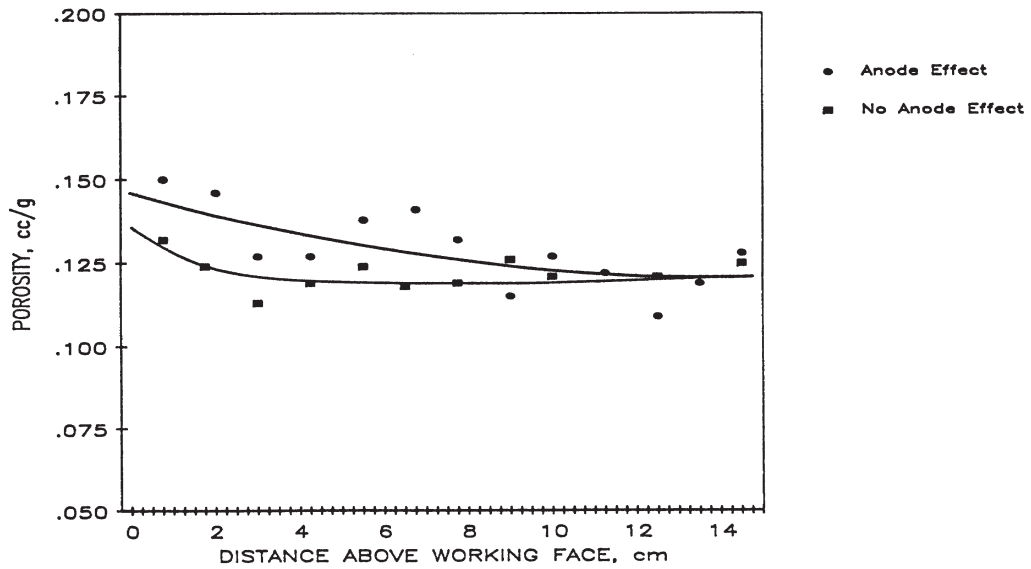


FIGURE 14.

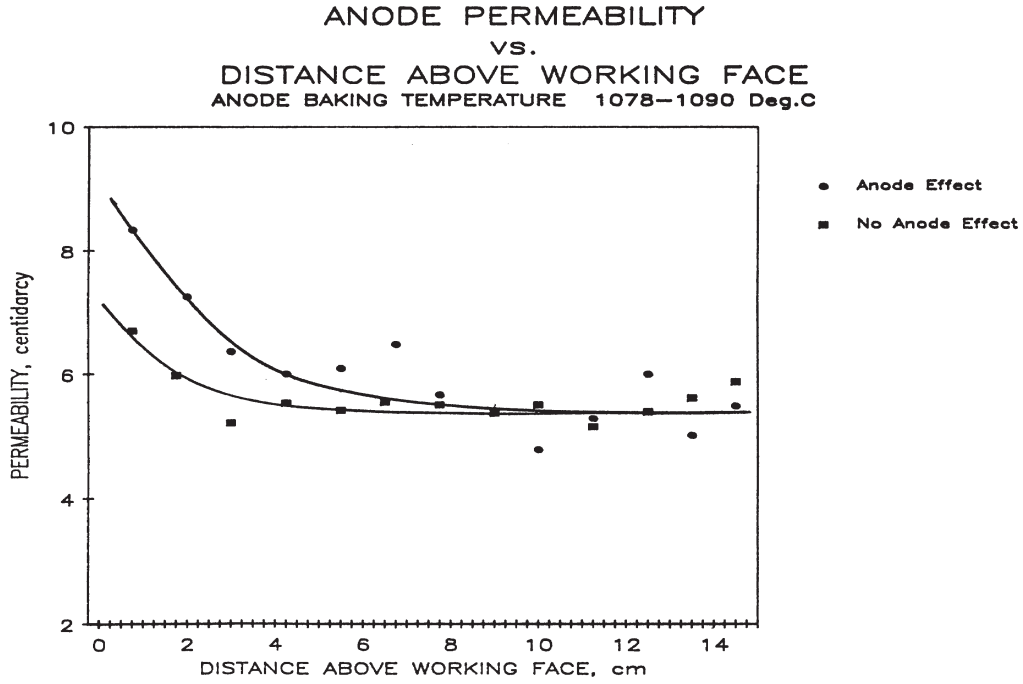


FIGURE 17.

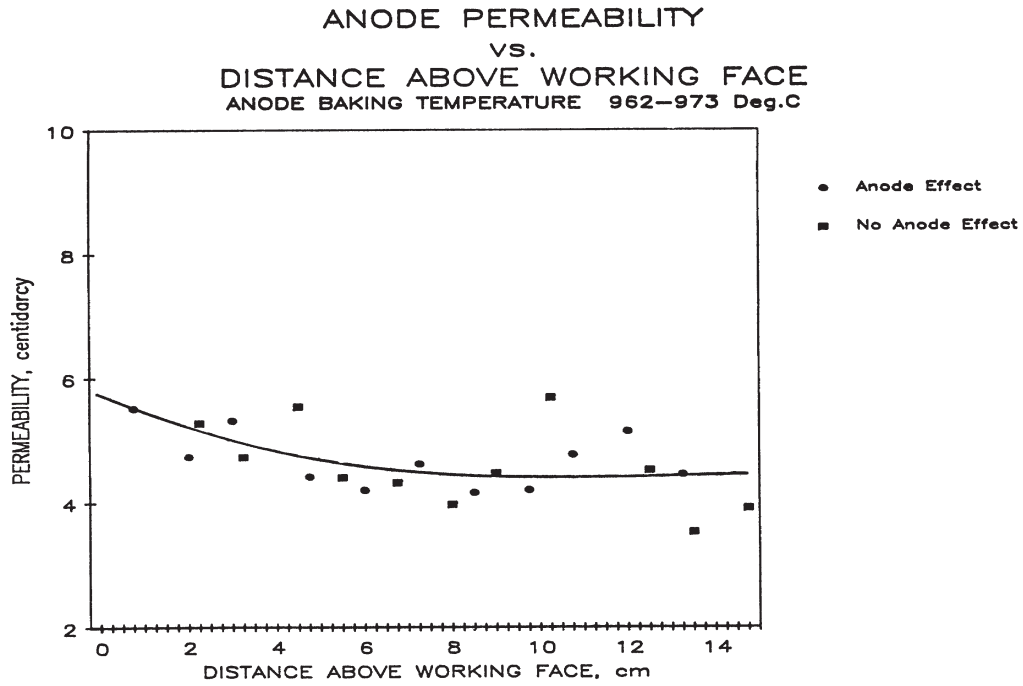


FIGURE 16.

ANODE SURFACE AREA  
vs.  
DISTANCE ABOVE WORKING FACE  
ANODE BAKING TEMPERATURE 962-973 Deg.C

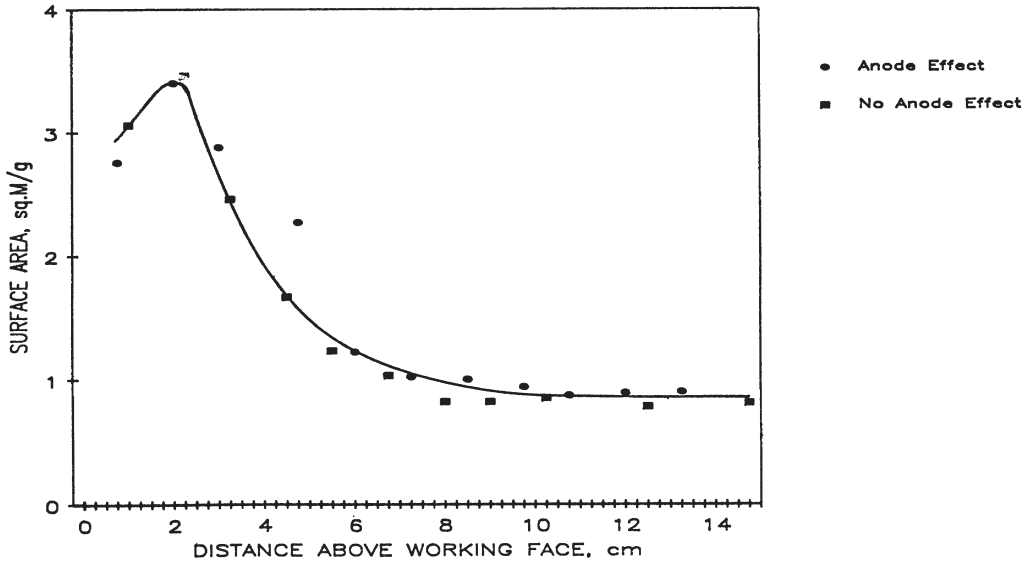


FIGURE 19.

ANODE SURFACE AREA  
vs.  
DISTANCE ABOVE WORKING FACE  
CONTROL BLOCKS (NOT ELECTROLYZED)

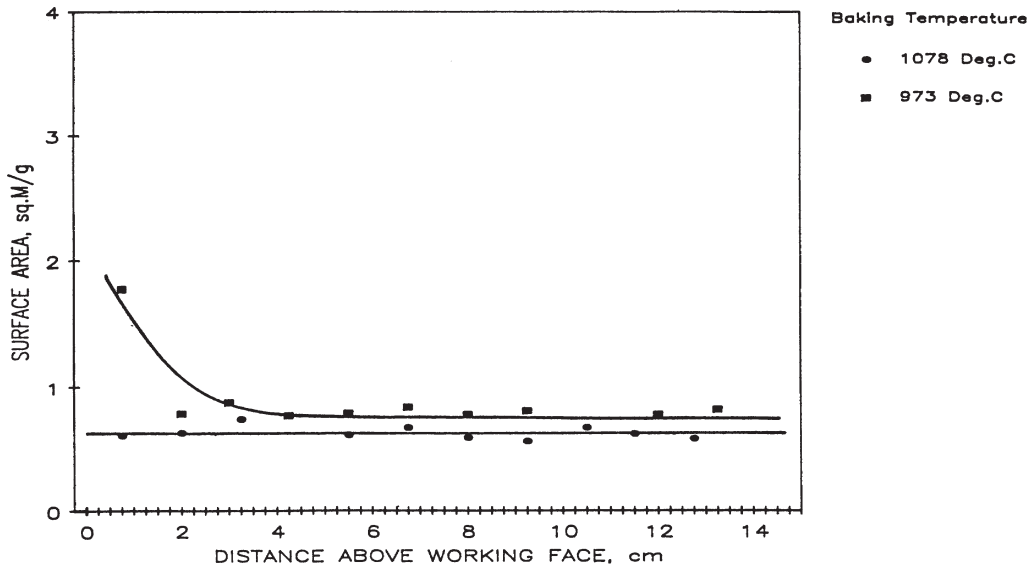


FIGURE 18.

did not experience an anode effect and (2) a block which was operated in the cell for two days at its normal current density and which experienced a 10-minute anode effect.

At the lower bake temperature, Figure 10, we see that apparent density is constant and the same as for non-electrolyzed blocks at distances greater than 5 cm above the working face. Below this distance, apparent density decreases due to the Boudouard reaction.



As is expected, apparent density is least for the carbon closest to the working face. What we really did not expect to see here is that the data from both anodes can be represented by the same line. In other words, for anodes baked to low temperatures no difference in apparent density is seen between a block which has had an anode effect and one which has not.

Now, consider Figure 11, blocks baked to a high temperature. We again see apparent density approaching the same value as that for the non-electrolyzed blocks; however, this time the effect shown on the graph reaches deeper into the blocks. Instead of 5 cm we see an increase anywhere from 7-10 cm above the working face and, also, the block which had an anode effect, generally speaking, has a lower apparent density than the one which did not.

#### Porosity

Figure 12 shows the porosity of the non-electrolyzed blocks. Although the data show some scatter, porosity is generally constant for both blocks. The higher temperature block, however, shows a higher overall porosity than the lower temperature block. This should be expected. The higher the baking temperature, the greater will be the shrinkage of the binder and, therefore, the greater the porosity.

For the low temperature blocks in Figure 13, the data for either block can generally be represented by a single line. For distances greater than 5 cm above the working face, the porosity remains constant; for distances less than 5 cm it increases due to the Boudouard reaction. Again, we see no contribution from the anode effect.

For the high temperature blocks in Figure 14, the situation is similar to that of apparent density. The block which experienced an anode effect showed a greater porosity as one approaches the working face than the block which did not.

#### Permeability

In Figure 15 the gas permeability of the non-electrolyzed blocks is constant at distances greater than 5-6 cm above the working face. However, permeability does decrease at closer distances to what would be the working face for these blocks. This decrease corresponds to an increase in apparent density. Both high and low temperature blocks show approximately the same permeability.

For the low temperature blocks in Figure 16, the scatter of the data is a bit worse than for porosity or apparent density. However, there is still no obvious difference between the block which did and did not experience an anode effect.

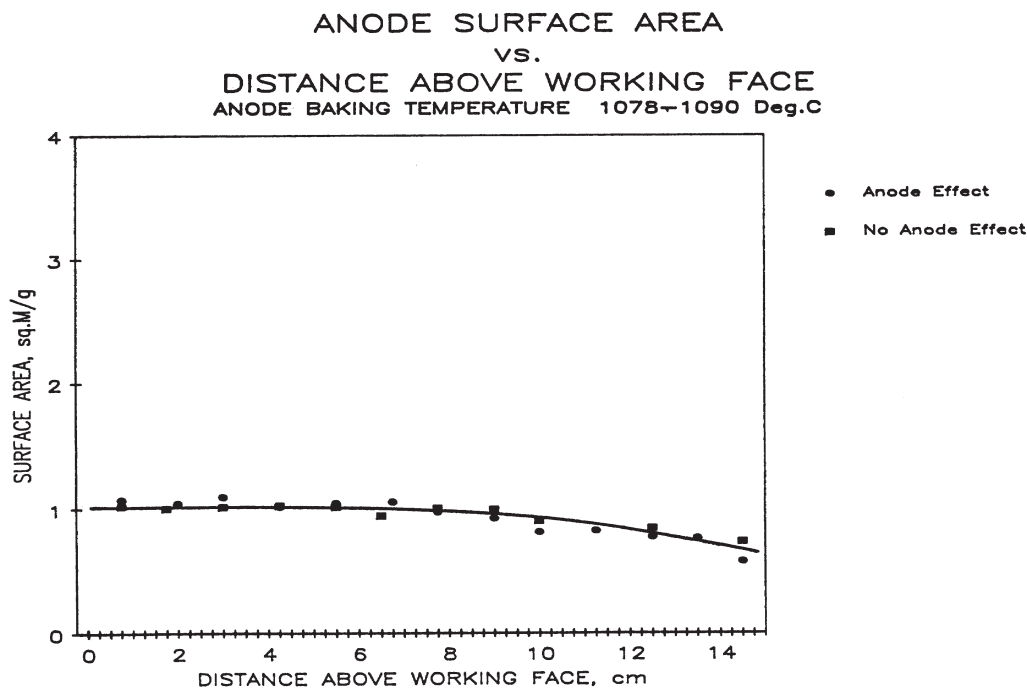


FIGURE 20.

The higher temperature blocks in Figure 17 show less scatter, and the data show a difference between the two blocks. As we approach the working face the permeability of both blocks increases. The block which had the anode effect shows a greater permeability than the one which did not.

#### Surface Area

The non-electrolyzed control blocks in Figure 18 show fairly constant surface area. The surface area of the low temperature block is slightly higher than that of the higher temperature block as would be expected based upon work already in the literature. The sharp increase in surface area of the low temperature block near the face is most probably due to air burning during baking, since this was a top layer block in the baking pit.

From Figure 19 the surface area of the low temperature blocks increases quite dramatically during operation as we move toward the anode face. For distances above 10 cm, the surface area is about the same as the control blocks. However, for values less than 10 cm above the face, we see that surface area has increased. This increase affirms that the Boudouard reaction is taking place; however, the data indicate that for low temperature blocks, it occurs as far as 10 cm into the anode rather than 5 cm which was indicated by our other data. Again, for the low temperature blocks the anode effect made no difference in surface area. Both blocks showed an increase in surface area when traveling toward the face with a slight decline around 2 cm.

In Figure 20 for the high temperature blocks, the surface area profile appears different; however, there is still nothing which indicates a change in block surface area between blocks having an anode effect and blocks which did not.

The large difference in surface area is seen between blocks baked at different temperatures, comparing Figures 19 and 20. We attribute this to the higher reactivity of the binder coke in the block baked to the low temperature.

#### Summary of Physical Properties

For the low temperature blocks no difference in any of the four properties was observed when comparing blocks which had and had not experienced an anode effect. For the high temperature blocks, differences in apparent density, porosity and permeability were observed. However, no difference was seen in surface area. This seems to be a bit puzzling, for if this were a true difference in properties, it would be more pronounced for blocks baked to a lower temperature. Since we did not see this for the lower temperature blocks, we can see no significant difference between any of the blocks which did and did not experience an anode effect. Thus, we can conclude that a single anode effect (although 10 minutes in duration) does not have an influence upon anode interior texture or sloughing. However, this is not to say that multiple anode effects do not influence the amount of carbon sloughed into the bath.

#### Surface Roughness

To this point we have only been concerned with the texture and properties of interior anode carbon. However, carbon sloughing is simply the process of loosening of aggregate by the selective burning of binder bridges. As the binder is selectively burned away the surface of the carbon becomes rougher. We believe a fair statement would be that the rougher the carbon surface is during electrolysis, the easier the aggregate

will be to remove and the greater will be the amount of carbon sloughed from the anode. Naturally, this assumes that the roughness is generated by electrolysis.

From the experimental anodes, we made two very interesting observations: (1) The working face of each anode was very hard and smooth. No carbon could be removed from this surface by rubbing one's hand on it. (2) The four sides of any of the anodes were much rougher than the working face, and aggregate particles could easily be removed by running one's fingers across the surface. Let us emphasize that this roughness was not generated by air burning. The portion of the anode side with which we were concerned was below bath level for the entire two-day duration of the experiment. Therefore, the majority of the carbon sloughed from these prebaked anodes is coming from the sides of the anodes, not the working face. Also, some anodes had sides much rougher with aggregate more easily removable than others. The relationship between surface roughness and anode properties is to be established below.

Surface roughness was measured for each anode by the method discussed in the previous section. The standard deviation of the particle depth measurements for each anode was used to indicate surface roughness. The data from these measurements are listed below in Table IX.

Table IX. Anode Surface Roughness

Baking Temperature, °C	Anode Effect	Surface Roughness, mm			
		Anode Side		Working Face	
		Average	Std. Dev.	Average	Std. Dev.
1080	No	1.2	0.43	-	-
1090	Yes	1.6	0.56	0.33	0.13
969	No	3.9	1.1	-	-
962	Yes	4.5	1.3	0.46	0.23

The side measured was the narrow one closest to the center of the pot. Along with the standard deviation, we have also listed the average pit depths, the "valleys". Notice that these pits vary from about 1 mm for a well baked anode to over 4 mm for a poorly baked anode. A picture of the side of each anode is shown in Figures 21 and 22. The high temperature anodes are shown in Figure 21 and the low temperature anodes in Figure 22. The electrolytic face of each anode is nearest the top of each photo. As you can easily see, the surface of the poorly baked anodes appears rougher than the well baked anodes. This supports the data shown in the previous table.

A graphical representation of the data in Table IX is shown in Figure 23. Again, the poorly baked anodes show a much greater degree of roughness than the well baked anodes. Also, the anodes which had an anode effect were slightly rougher than the corresponding temperature anodes which did not. This difference, though, is nowhere near as great as the effect of baking temperature. Also shown are roughness measurements for the electrolytic face of two of the anodes. The face of the other two anodes had a coating of bath which prevented accurate measurements. You can easily see that the face of both of these anodes is much smoother than the sides. All of these values and their graphical representation bear out our observations on the anodes. The face was very hard and intact. No



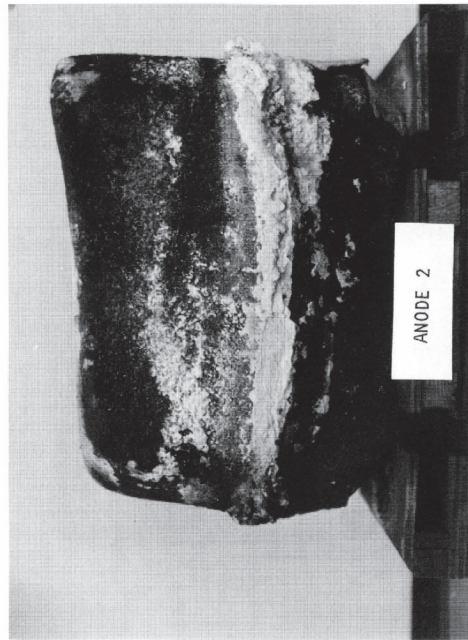
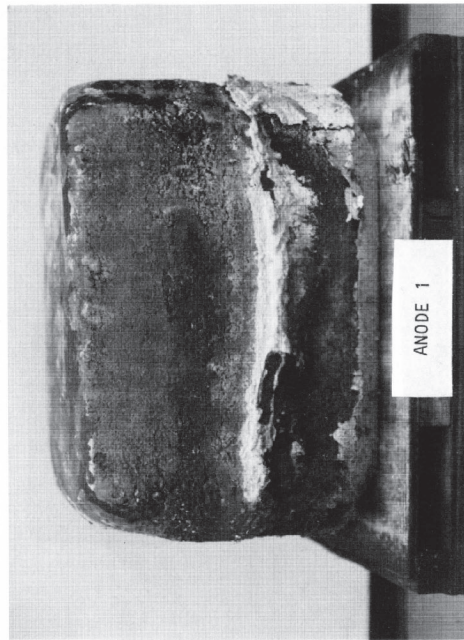


FIGURE 21.  
HIGH TEMPERATURE ANODES

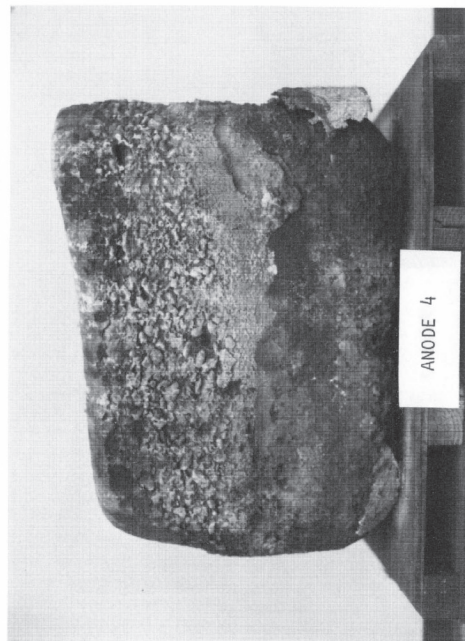


FIGURE 22.  
LOW TEMPERATURE ANODES

aggregate particles could be removed by brushing the surface with one's fingers. The anode sides were another matter. Aggregate particles were easily loosened and fell off. The particles were much easier to remove from the poorly baked anode than from the well baked anode. We could tell no difference between the anodes which did and did not experience an anode effect.

The conclusions we draw from this data are that concerning baking temperature and anode effects, baking temperature is definitely the more important property contributing to sloughing. A single anode effect may tend to contribute to sloughing but to a much lesser degree than baking temperature.

#### In summary,

1. Surface area measurements indicate that electrolytically generated CO<sub>2</sub> penetrates the first 8-10 cm above the working face of active anodes consuming interior anode carbon.
2. Data indicate that a single anode effect has little influence upon carbon sloughing; this is not to say that multiple anode effects have the same small influence.
3. Anode baking temperature has more influence upon carbon sloughing than a single anode effect. A poorly baked anode will produce more slough carbon than a well baked one. A distinct difference between well and poorly baked anodes can be seen in relation to anode working face surface area and anode side surface roughness.
4. The majority of carbon sloughed from an anode should originate from the sides of that anode rather than the working face.

#### References

1. Paul Rhede, *Light Metals 1971*, pp. 385-408.
2. Jomar Thonstad, Paper Presented at International Meeting on Anode Problems in Aluminum Electrolysis, Milan, June 7-9, 1971.
3. O. Bowitz, et al, *First Conference on Industrial Carbon and Graphite*, 1957, p. 373.
4. E. A. Hollingshead and V. A. Braunwarth, *Extractive Metallurgy of Aluminum*, 1963, pp. 31-49.
5. T. Watanabe, *Extractive Metallurgy of Aluminum*, 1963, pp. 351-372.
6. Elektrokemisk, A/S, BP 746,625.
7. H. C. Fritz and R. E. Gehlbach, Paper Presented at the 111th AIME Annual Meeting, Feb. 14-18, 1982, Dallas.
8. G. J. Houston, "A Survey of Anode Consumption in Hall-Heroult Cells," Institute of Inorganic Chemistry, Norwegian Institute of Technology, p. 41.
9. O. Bowitz, et al, *Extractive Metallurgy of Aluminum*, 1963, pp. 331-349.

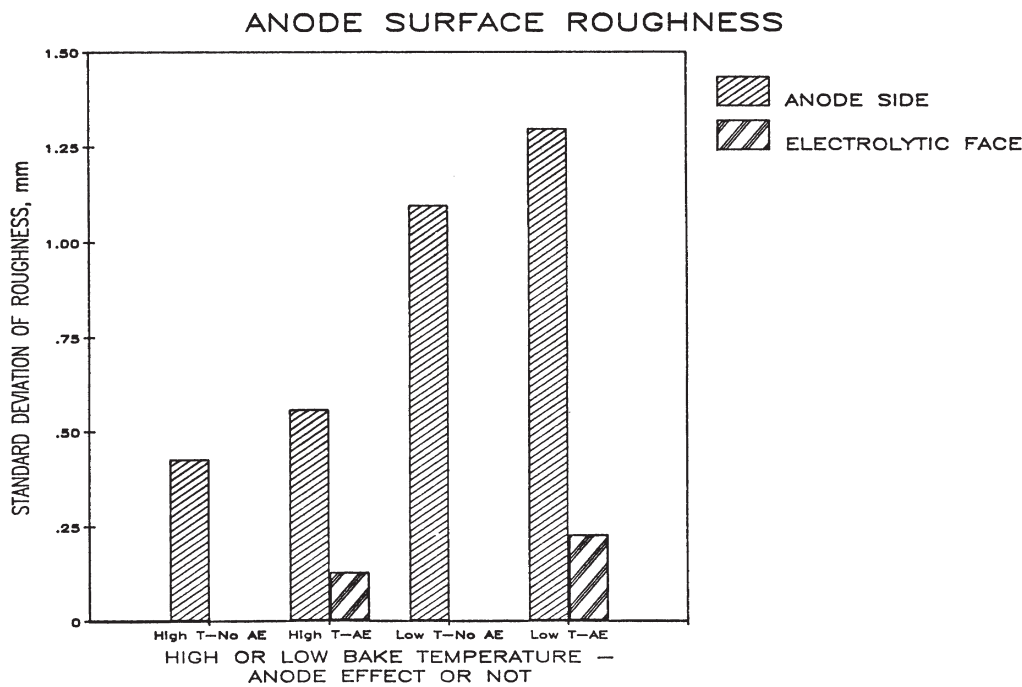


FIGURE 23.

10. E. Barrillion, Paper Presented at International Meeting on Anode Problems in Aluminum Electrolysis, June 7-9, 1971.
11. E. Barrillion, Light Metals 1971, pp. 351-364.
12. R. Boero, Light Metals 1981, pp. 441-458.
13. R. Farr-Wharton, et al, Electrochimica Acta, 25, p. 217, 1980.
14. A. Paulin, "Structure of Anodes and Gas Flow Through Anodes in Electrolysis of Aluminum," Yugoslav Symposium on Aluminum, Vol. 1, 166 (1978).
15. B. P. Dormachew and M. A. Korobov, Tsvetnye Metally, December 1971, p. 30.
16. B. I. Ayushin, et al, Tsvetnye Metally, 1977, p. 44.

#### Appendix

##### Experimental Technique Used to Determine Anode Physical Properties

#### 1. Apparent Density

For each slice of the anode cores which were analyzed the dimensions, thickness and diameter, were measured to the nearest 0.001 inch. The slice was weighed to the nearest 0.01 gram. Apparent density was calculated as follows:

$$\text{Apparent Density} = \frac{\text{Mass}}{\text{Volume}}$$

#### 2. Porosity

A piece, 1 cm x 1 cm x 0.5 cm, was cut from each slice. An American Instrument Company mercury intrusion porosimeter was used to determine total pore volume. Maximum pressure used was 10,000 psi representing pores with diameters of 0.017 micron or larger. Total pore volume was then reduced to pore volume per gram of sample.

#### 3. Permeability

Gas permeability was determined for each 2 in. dia. x 1 cm thick slice using a permeameter manufactured by Porous Materials, Inc. CO<sub>2</sub> was chosen as the permeating gas. Permeability was calculated using the following equation:

$$K = \frac{800 Q_0 P_0 L \mu}{(P_i^2 - P_o^2) \pi D^2}$$

K = Permeability, centidarcy  
 Q<sub>0</sub> = Flow rate of CO<sub>2</sub>, cm<sup>3</sup>/sec.  
 L = Length of sample, cm  
 μ = Viscosity of CO<sub>2</sub>, centipoise  
 P<sub>i</sub> = Inlet pressure, absolute, atmospheres  
 P<sub>o</sub> = Outlet pressure, absolute, atmospheres  
 D = Sample diameter, cm

#### 4. Surface Area

A Quantachrome, Inc. Monosorb surface area instrument was used. Surface area was determined using a 1 cm x 1 cm x 2 cm sample from each slice and calculated using the B.E.T. equation. Nitrogen gas was used as the adsorbent.